Turkish Journal of Electrical Engineering & Computer Sciences

http://journals.tubitak.gov.tr/elektrik/

Research Article

Turk J Elec Eng & Comp Sci
(2023) 31: 17 – 38
© TÜBİTAK
doi:10.55730/1300-0632.3968

Deep learning-based classification of chaotic systems over phase portraits

Sezgin KAÇAR[1,*], **Süleyman UZUN**[2], **Burak ARICIOĞLU**[1]

[1]Department of Electrical and Electronics Engineering, Faculty of Technology, Sakarya University of Applied Sciences, Sakarya, Turkey

[2]Department of Computer Engineering, Faculty of Technology, Sakarya University of Applied Sciences, Sakarya, Turkey

Received: 09.12.2021 • **Accepted/Published Online:** 13.06.2022 • **Final Version:** 19.01.2023

Abstract: This study performed a deep learning-based classification of chaotic systems over their phase portraits. To the best of the authors' knowledge, such classification studies over phase portraits have not been conducted in the literature. To that end, a dataset consisting of the phase portraits of the most known two chaotic systems, namely Lorenz and Chen, is generated for different values of the parameters, initial conditions, step size, and time length. Then, a classification with high accuracy is carried out employing transfer learning methods. The transfer learning methods used in the study are SqueezeNet, VGG-19, AlexNet, ResNet50, ResNet101, DenseNet201, ShuffleNet, and GoogLeNet deep learning models. As a result of the study, classification accuracy between 97.4% and 100% for 2-ways classifier and between 83.68% and 99.82% for 3-ways classifier is achieved depending on the problem. Thanks to this, random signals obtained in real life can be associated with a mathematical model.

Key words: Chaotic systems, phase portraits, classification, deep learning, transfer learning

1. Introduction

Chaotic systems and chaotic behaviors are a subfield of nonlinear systems. Studies on the classification of chaotic signals with artificial intelligence methods have just begun to emerge [1]. Most systems in our physical world have nonlinear mathematical models, as we all know. As previously stated, one of the behavioral characteristics of nonlinear systems is that they can exhibit chaotic behavior based on system parameters and initial values [2, 3]. Chaotic systems are systems that exhibit chaotic behavior at this point. The Lorenz system was chosen as the first of the systems discussed in our study because it was one of the first studies on the subject and one of the most well-known [2, 3]. Because the goal of the study is to classify systems based on the chaotic signals they generate, two different systems are discussed, one similar to the Lorenz system and the other with a different structure. Because of its widespread use in the literature [4, 5], the Chen system, which is derived from the Lorenz system as a system similar to the Lorenz system, and the Rössler system as a different system, has been preferred. As a result, the performance of the model developed in the classification problem is comparable, and its performance is measured on various systems. The purpose of classifying with the phase portrait in this study is to make classifications based on the relationship between the state variables appearing in the phase portraits, rather than only on time series based on a single state variable. As a result, it aims to outperform classifications performed on similar time series in different systems. Another reason for using phase portraits in the study is to contribute to the literature, as this approach has not previously been used in similar studies.

*Correspondence: skacar@subu.edu.tr

The findings show that this approach is more effective, particularly in the transfer learning method.

In recent years, chaos or chaotic systems have been employed in various fields in engineering such as secure communication [6], data security [7], cryptography [8], video and audio encryption [9, 10], weak signal detection [11], random number generators [12], digital signature applications [13], and DC-DC converters [14]. Moreover, deep learning has become one of the most popular literature topics in recent years [15]. Despite the fact that there are many studies on deep learning, these studies are usually on the classification processes of different fields. In this study, the two of the most famous subjects, namely chaos and deep learning, are considered, and deep learning-based classification of the phase portraits of the chaotic systems is carried out.

Deep learning is a part of machine learning [16] that employs multilayer artificial neural networks on several engineering applications such as image processing [17, 18], voice recognition [19, 20], natural language processing [21–23], and object recognition [24]. In deep learning, the learning process can be achieved autonomously as opposed to traditional machine learning algorithms in which the learning process can be achieved with fixed rules [25]. To the best of the authors' knowledge, there is no deep learning-based classification study on the images of phase portraits of chaotic systems. On the other hand, deep learning-based classification of the chaotic signals over time series is available in the literature.

The work carried out by Boulle et al. [26] is one of the most promising works performed in this area. In that work, the classification of time series of discrete and continuous-time dynamical systems was performed by employing ShallowNet, multilayer perceptrons (MLP), the fully convolutional neural network (FCN), residual network – ResNet, large kernel convolutional neural network (LKCNN) methods. It was found out that the highest classification performance was observed with LKCNN method. In Uzun's study [27], the time series of Lorenz, Chen, and Rössler systems, three of the well-known chaotic systems, are classified using machine learning algorithms. As classification success, it was obtained with the K-Nearest Neighbor algorithm with 99.20% success. Yeo [28] employed the long short-term memory network (LSTM) in his study of prediction of chaotic system from noisy observation. It was concluded that LTSM filters out noise effectively, and this enables achieving of high accuracy prediction of nonlinear dynamics. Kuremoto et al. [29] generated deep belief nets (DBNs) by employing restricted Boltzmann machine (RBM) and multilayer perceptron (MLP) for the prediction of the time series of the Lorenz and Henon map systems. They concluded that their generated DBNs have better prediction accuracy than the traditional DBNs. Sangiorgio et al. [30] classified the noiseless time series of the chaotic systems with their proposed methods. These methods are feed-forward (FF)-recursive, FF-multi-output, LSTM-teacher forcing (TF), and LSTM-no-TF. They concluded that LTSM based predictors have superior performance than FF-recursive and FF-multi-output methods.

The main goal of this research is to show that phase portraits can be used to classify similar and dissimilar chaotic systems. The results show that this classification can be done quickly and accurately. If any physical system is found to exhibit chaotic behavior, it will be possible to determine which chaotic system model the system has, or at least convergence, over the phase portraits of the experimentally obtained time series, without the need for mathematical modeling. The research presented here should be regarded as a preliminary study for the abovementioned applications.

In the literature, there are not many studies about the deep learning-based classification of chaotic signals, and there is not any study at all regarding deep learning-based classification chaotic systems over their phase portraits images. In this study, a high accuracy classification of the chaotic systems is performed using the most common deep learning models of SqueezeNet[31], VGG-19[32], AlexNet[33], ResNet50[34], ResNet101[34], DenseNet201[35], ShuffleNet[36], and GoogLeNet[37]. To the best of the authors' knowledge, a high accuracy classification of different chaotic systems over phase portrait images is presented for the first time in the literature. The advantages of using transfer learning can be listed as follows despite the situation of obtaining a new model by training from scratch;

-Provides faster training time as they contain a lot of information extracted from model images used in transfer learning.

-One of the biggest disadvantages is the need for large-scale data in model building applications from scratch. On the other hand, in transfer learning models, classification can be made with less data with higher accuracy.

-The performance of transfer learning models can be increased by performing simple operations such as adding full link layers to their structures.

The paper is so organized that Section 2 presents the used chaotic systems and data sets obtained from these chaotic systems. Section 3 presents the used deep learning models. Section 4 presents the classification processes and their performance results, and Section 5 offers the conclusion.

2. The used chaotic systems and obtained dataset

Lorenz, Chen, and Rössler chaotic systems are considered in this study. There are many different chaotic systems available in the literature. These three systems are selected because they are the most common chaotic systems [38] and three-dimensional, contain similar nonlinear terms in their mathematical model, and can be used to model physical systems such as atmospheric, electrical and chemical systems. Moreover, these three systems are selected because the time series and phase portraits of Lorenz and Chen systems are very alike, while the time series and phase portraits of Rössler system are very different than those of Lorenz and Chen systems. The Rössler chaotic system has a completely different mathematical model than the others. Lorenz and Chen have mathematical models that are very similar. This makes the selection of these three systems logical for the classification performance evaluation purpose. A data set is constructed using time series and phase portraits of these three chaotic systems.

2.1. Lorenz system

Edward Lorenz proposed the Lorenz system in 1963 as a simplified mathematical model of atmospheric convection [39, 40]. Lorenz system is a system of three ordinary differential equations as given in Equation 1. Here, x, y, and z represent the state variables, and a, b, and c represent the system parameters.

$$\begin{aligned}\dot{x} &= ay - ax\\ \dot{y} &= xc - xz - c\\ \dot{z} &= xy - bz\end{aligned} \tag{1}$$

Moreover, the Lorenz system can also be in the modeling of thermosiphons [41], lasers [42], electrical circuits [43], brushless DC motors [44], dynamos [45], and chemical reactions [43]. Figure 1 shows the time series and phase portraits of the Lorenz chaotic system for the system parameters a = 10, b = 8/3, c = 28, initial conditions x0 = 1, y0 = –1 and z0 = 1.5. The time series given in Figure 1 has random variations. The chaotic systems can be used in encryption and data security applications thanks to this randomness property of the chaotic signals.

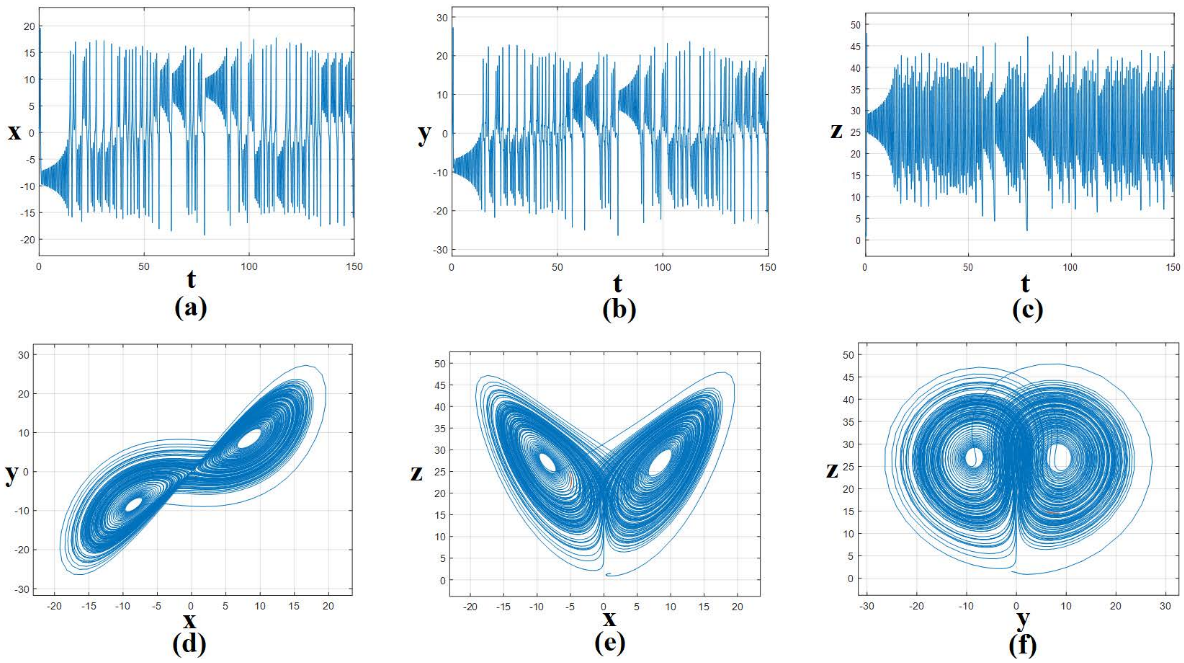

Figure 1. Time series and phase portraits of the Lorenz system for system parameters a = 10, b = 8/3, c = 28 and x0, y0, z0 = 1, –1, 1.5. (a) Time series of x, (b) Time series of y, (c) Time series of z, (d) Phase portrait of x-y, (e) Phase portrait of x-z, (f) Phase portrait of y-z.

2.2. Chen system

Guanrong Chen and Ueta have introduced a double scrolled chaotic system called the Chen system or Chen chaotic attractor in 1999 [46, 47]. Chen system is a system of three ordinary differential equations as given in Equation 2. Here, x, y, and z represent the state variables, and a, b, and c represent the system parameters.

$$\begin{gathered}\dot{x} = ay - ax \\ \dot{y} = cx - ax - xz + cy \\ \dot{z} = xy - bz\end{gathered} \tag{2}$$

Figure 2 shows the time series and phase portraits of Chen chaotic system for the system parameters a = 40, b = 3, c = 25, initial conditions x0 = 0.2, y0 = 0.5 and z0 = 0.8. If the time series phase portraits given in Figures 1 and 2 and the equation systems given in Equations 1 and 2 are examined, it can be said that the Lorenz and Chen systems have some similarities. These similarities will be a challenge to be overcome for the classification process.

2.3. Rössler system

Otto Rössler developed the Rössler system in 1976, which can be very useful for modeling chemical reactions [48, 49]. Rössler system is a system of three ordinary differential equations as given in Equation 3. Here x, y, and z represent the state variables, and a, b, and c represent the system parameters.

$$\begin{gathered}\dot{x} = -y - z \\ \dot{y} = x + ay \\ \dot{z} = zx - zc + b\end{gathered} \tag{3}$$

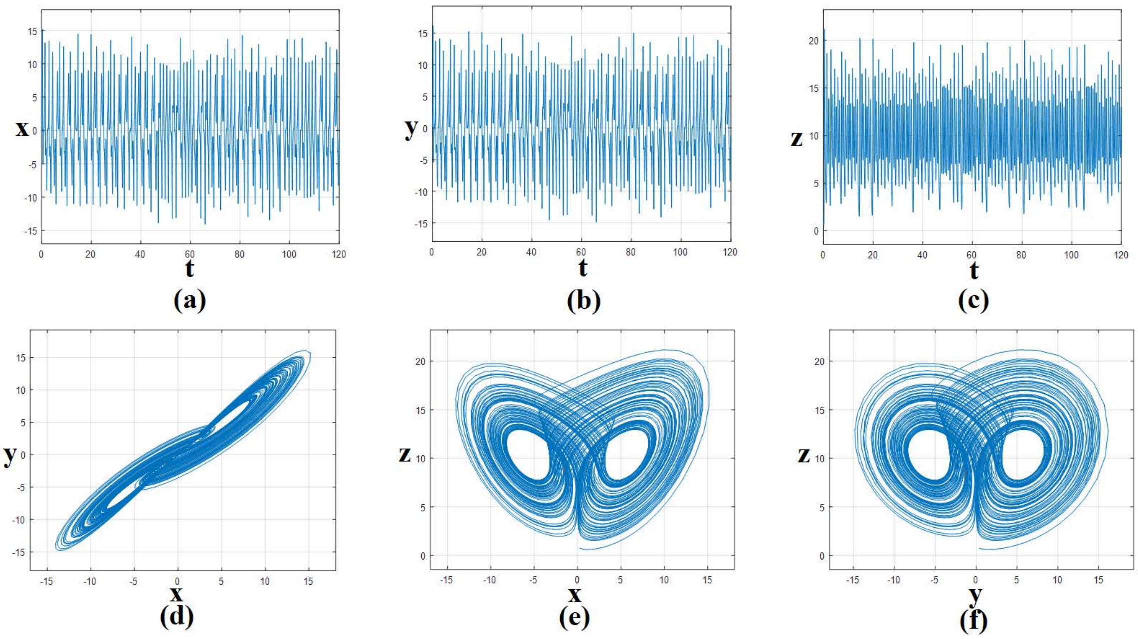

Figure 2. Time series and phase portraits of the Chen system for system parameters a = 40, b = 3, c = 25 and x0, y0, z0 = 0.2, 0.5, 0.8. (a) Time series of x, (b) Time series of y, (c) Time series of z, (d) Phase portrait of x-y, (e) Phase portrait of x-z, (f) Phase portrait of y-z.

The Rössler system is a single scroll system that can be easier to analyze than the Lorenz system, even though their equation systems are similar. Figure 3 shows the time series and phase portraits of Rössler chaotic system for the system parameters a = 0.1, b = 0.1, c = 14, and initial conditions x0 = 12, y0 = 12 and z0 = 0. The time series and phase portraits of the Rössler system are very different than those of the other two systems. This makes the classification of the Rössler system easier. Thus, the classification performance will be evaluated on an elementary problem.

2.4. The produced dataset

In this section, how the data set is generated is presented. Before generating the data set, the three chaotic systems were solved numerically with Runge-Kutta 4 (RK4) algorithm [50] to obtain state variables of the chaotic systems. Runge-Kutta is one of the most widely used and fundamental methods for solving ordinary differential equations systems numerically. The RK4 algorithm, as shown in Equation 4, is a method that can converge to the correct result with a small number of errors. The state variables are calculated for different system parameters and initial conditions values. Moreover, the length of time series (or the number of calculated points) and the step size of the RK4 algorithm are also varied for generating the data set.

$$\begin{aligned} RK_1 &= kf(a_i, b_i) \\ RK_2 &= kf(a_i + \tfrac{k}{2}, b_i + \tfrac{t_1}{2}) \\ RK_3 &= kf(a_i + \tfrac{k}{2}, b_i + \tfrac{t_2}{2}) \\ RK_4 &= kf(a_i + k, b_i + t_3) \\ b_{i+1} &= b_i + \tfrac{t_1}{6} + \tfrac{t_2}{3} + \tfrac{t_3}{3} + \tfrac{t_4}{6} + O(k^5) \end{aligned} \tag{4}$$

Then phase portraits are obtained after calculating the state variables. For every variable of a chaotic system, 750 different time series data were calculated. Since all the chaotic systems are 3-dimensional, 2250 different time series are calculated for each chaotic system, and the total 6750 different time series are calculated for the three chaotic systems. The system and calculation parameter values are as shown in Table 1. All the phase portraits are saved as a 128 × 128-pixel image because the transfer learning methods are very useful for image classification. The data set consists of 6750 different phase portraits images.

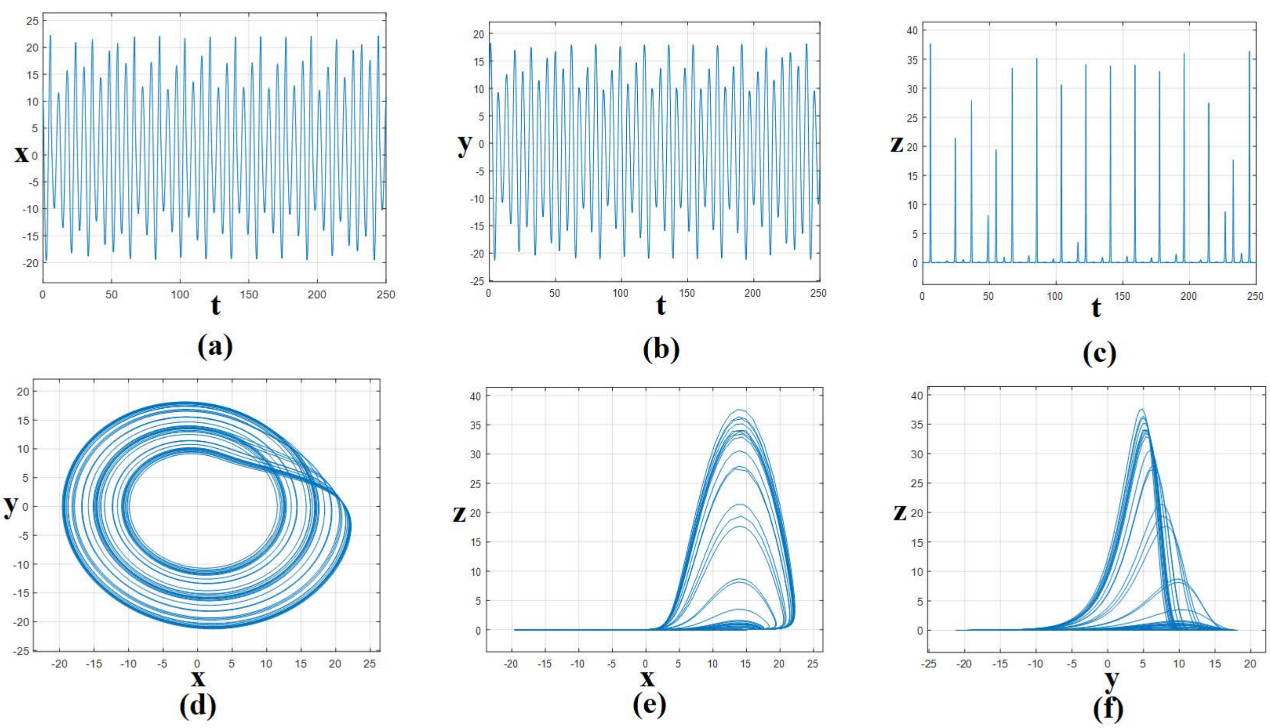

Figure 3. Time series and phase portraits of the Rössler system for system parameters a = 0.1, b = 0.1, c = 14 and x0, y0, z0 = 12, 12, 0. (a) Time series of x, (b) Time series of y, (c) Time series of z, (d) Phase portrait of x-y, (e) Phase portrait of x-z, (f) Phase portrait of y-z.

Table 1. The used calculation parameters for dataset.

System	System parameters (Only b parameters are changed for every system)	The length of time series (the number of total calculated points)	The step size of RK4 algorithm	The Initial conditions
Lorenz	b=2.5, 3, 3.5, 4, 4.5, 5	10000, 12500, 15000, 17500, 20000	0.01 0.02 0.05 0.1 0.2	X0=0.1, 0.2, 0.3, 0.4, 0.5 Y0=0.3, 0.4, 0.5, 0.6,0.7 Z0=0.4, 0.5, 0.6, 0.7, 0.8
Chen	b=0.05, 0.1, 0.15, 0.2, 0.25, 0.3	20000, 25000, 30000, 35000, 40000		X0=8, 9, 10, 11, 12 Y0=8, 9, 10, 11, 12 Z0=0, 1, 2, 3, 4
Rössler	b=2.5, 2.55, 2.6, 2.65, 2.7, 2.75	2000, 4000, 6000, 8000, 1000		X0=8, 9, 10, 11, 12 Y0=-8, -9, -10, -11, -12 Z0=13, 14, 15, 16, 17

3. The used deep learning models

In this study, deep learning-based classification of three different chaotic systems over their xy, yz, and xz portraits are presented. The classification is carried out by applying eight different pretrained deep learning models (VGG-19, AlexNet, ResNet50, ResNet-101, DenseNet-201, ShuffleNet, and GoogLeNet) on the phase portrait images of the three chaotic systems.

3.1. Deep learning and convolutional neural networks (CNN)

As seen in Figure 4, deep learning is a subcategory of machine learning algorithms that employ different architectures to learn the distinctions on the data [51]. Artificial neural network-based deep learning algorithms have multilayer neural networks to accomplish the learning process [52, 53].

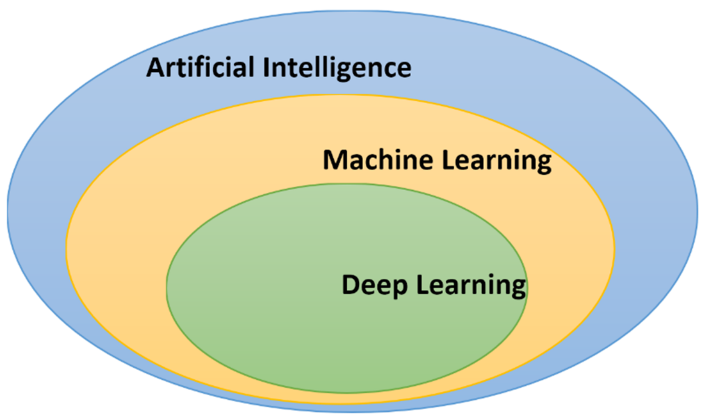

Figure 4. The relationship between deep learning, machine learning and artificial intelligence.

In traditional machine learning algorithms are developed to analyze data with very few numbers of features. The traditional machine learning algorithms are not feasible to analyze data sets with numerous features. To overcome this drawback, CNN is developed. The size of image data is high, and each image consists of a significant number of pixels. Because of this, CNNs achieve much higher performance than traditional machine learning algorithms for analyzing such data sets [54].

In 1988, LeNet networks were proposed to process images of large size by Lecun et al. This network is considered as the first CNN network [55, 56]. The consecutive sublayers of convolutional and maximum pooling layers constitute LeNet networks. The next top layers are the ones corresponding to MLP. In this network, the average errors of predicted and obtained results are minimized by training the weights of the network [54].

There are many different network models of CNN available in the literature. SqueezeNet, VGG-19, AlexNet, ResNet50, ResNet-101, DenseNet-201, ShuffleNet, and GoogLeNet are some of the example architectures of these models [57]. These pretrained networks can enable faster processing in the CNN models, increase classification performance and increase learning process speed. The performance of these networks varies according to the problem they handle. Thus, according to the problem, the pretrained network with the highest performance is preferred. In this study, these pretrained networks are applied and tested, and among them, the networks with higher performance are used.

3.2. ResNet50 and ResNet101

The network architecture of ResNet50 contains 152 layers. It won the ImageNet 2015 contest [34]. The architecture contains convolution, activation, pooling, and fully connected layers. ResNet architecture is given in Figure 5. There are five convolutional blocks, each containing 1 × 1, 3 × 3, and 1 × 1 convolutional layers in the network structure [58, 59]. The size of images is shrunken by the global averaging layer and process of the two-step sampling [60]. Softmax is the activation function of the fully connected layers.

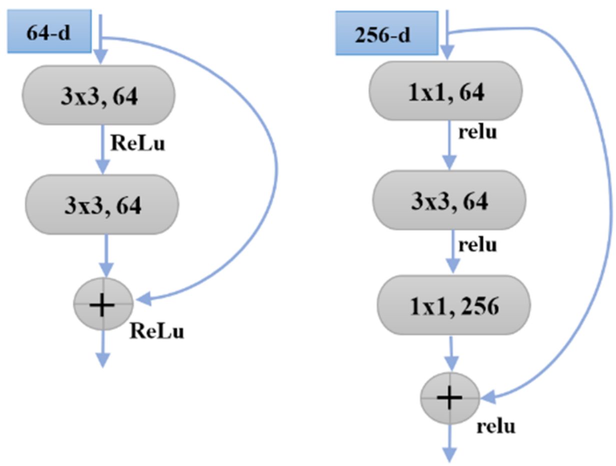

Figure 5. Training sample of the ResNet architecture with residual layers [34].

3.3. SqueezeNet

SqueezeNet CNN network was introduced in 2016. SqueezeNet architecture is given in Figure 6. Its architecture is constructed by improving AlexNet architecture. The main difference between AlexNet and SqueezeNet is the former has 240MB of parameters while the latter has 5MB of parameters.

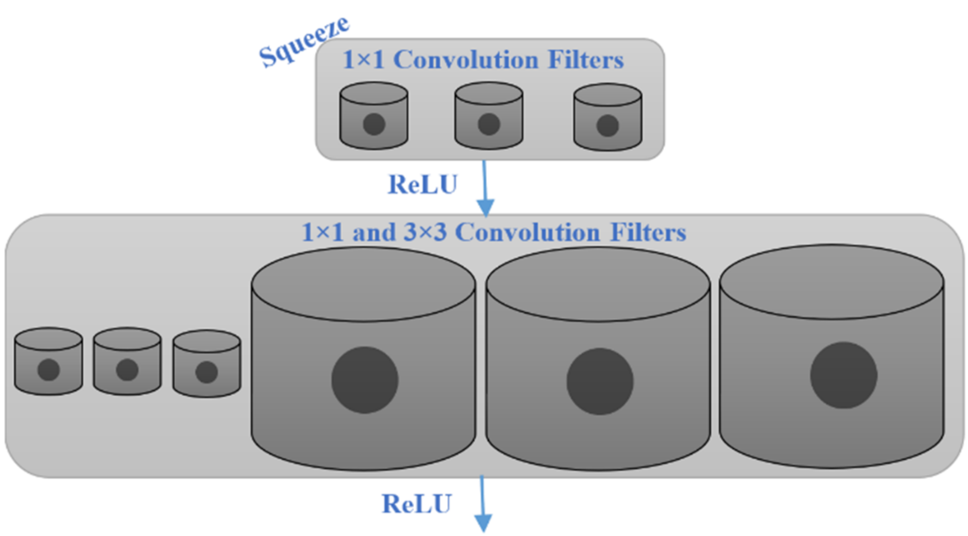

Figure 6. SqueezeNet network fire module [31].

The performance of SqueezeNet is as good as that of AlexNet. SqueezeNet also contains fire layers. SqueezeNet as which show Figure 7 also contains Fire layers. In this layer, filters size is reduced to 1 × 1 in order to decrease the number of calculated features [31]. Hence, the workload of the neural network decreased, and SqueezeNet performs faster [61].

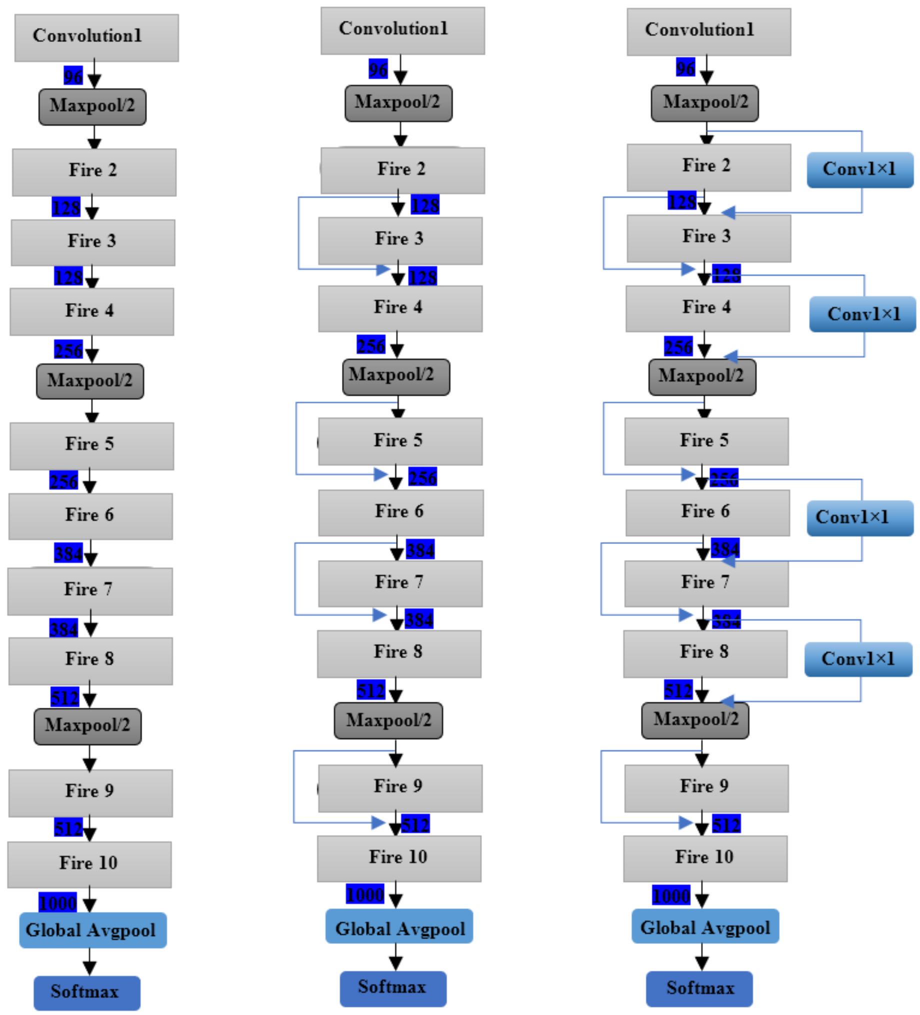

Figure 7. The structure of squeezenet network [31].

3.4. AlexNet

Krizhevsky et al. proposed AlexNet as a CNN network in 2012 [33, 62]. Its architecture contains consecutive convolutional, max-pooling and fully connected layers, and its activation function is rectified linear unit (ReLU) [63]. AlexNet is usually employed in the classification of images [64]. AlexNet architecture is given in Figure 8 [65].

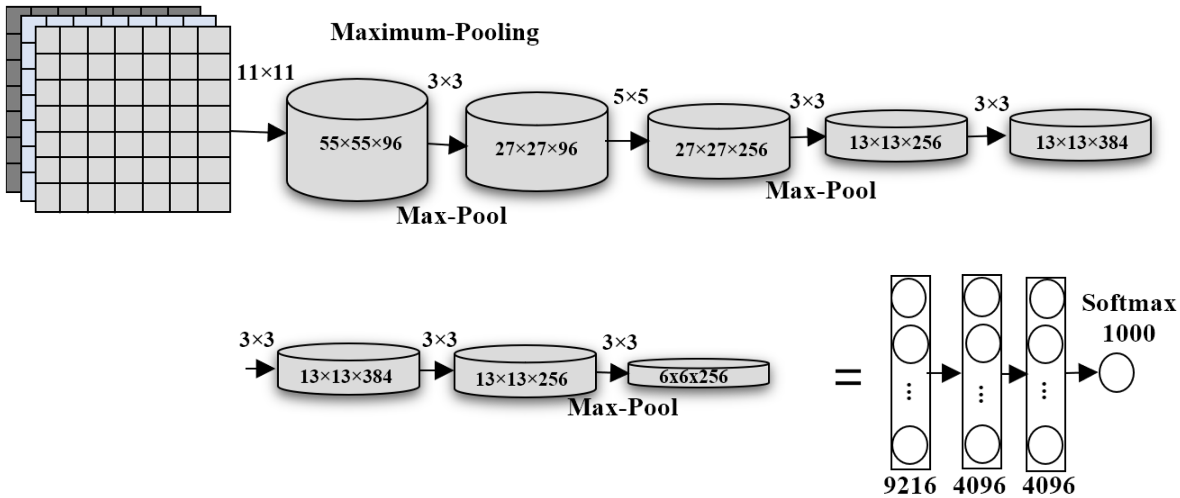

Figure 8. The architecture of AlexNet network [65].

3.5. DenseNet-201

DenseNet is a convolutional neural network with its dense connection model. The DenseNet architecture has inputs of 224 × 224 × 3 sized images as shown in Figure 9 [66].

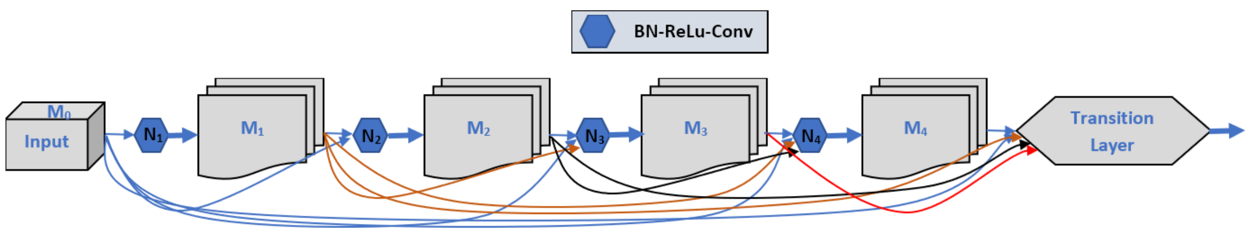

Figure 9. The structure of DenseNet network [66].

The architecture's dense blocks contain normalization, ReLU and 3 × 3 convolutional layers [67]. DenseNet architecture connects the layers instead of adding up as in the previous architectures like ResNet. In the connection layers, all the extracted features in the previous layer are combined and transferred to the next layer. In DenseNet, the excess features maps are removed while transferring them to the next layer in order to prevent retraining of the excess features in the next layers. On the other hand, this is not valid for the other network architectures [35, 68].

3.6. ShuffleNet

Zhang et al. designed ShuffleNet for mobile devices with limited processing power. ShuffleNet is a CNN model which has quite good performance [36, 69]. This network retains accuracy while decreasing computational cost. In addition, it has much higher performance than other architectures on studies of ImageNet classification and MS COCO object recognition [36]. The architecture of ShuffleNet is given in Table 2.

As seen in Table 2, the network model consists of ShuffleNet stack units, which are grouped in three stages. In each stage, the first block of all structures begins with two strides. While some parameters in one stage remain the same, the output channels are double for the next stage. The group number g given in Table 2 controls the connection sparsity of pointwise convolutions.

Table 2. ShuffleNet architecture.

Layer	Output size	K size	Stride	Repeat	Output Channels (g groups)				
					g=1	g=2	g=3	g=4	g=8
Image	224 × 224				3	3	3	3	3
Conv1	112 × 112	3 × 3	2	1	24	24	24	24	24
MaxPool	56 × 56	3 × 3	2						
Stage2	28x28		2	1	144	200	240	272	384
	28 × 28		1	3	144	200	240	272	384
Stage3	14 × 14		2	1	288	400	480	544	768
	14 × 14		1	7	288	400	480	544	768
Stage4	7 × 7		2	1	576	800	960	1088	1536
	7 × 7		1	3	576	800	960	1088	1536
GlobalPool	1 × 1	7 × 7							
FC					1000	1000	1000	1000	1000
Complexity					143M	140M	137M	133M	137M

3.7. GoogLeNet

GoogLeNet, proposed by Szegedy et al., contains 22 layers. GoogLeNet is a pretrained CNN and was selected as the most successful network in the contest of ILSVRC2014 [37, 64, 70]. The architecture of the network is shown in Figure 10. In the architecture, there are parallel connected layers for minimizing the possibility of memorization.

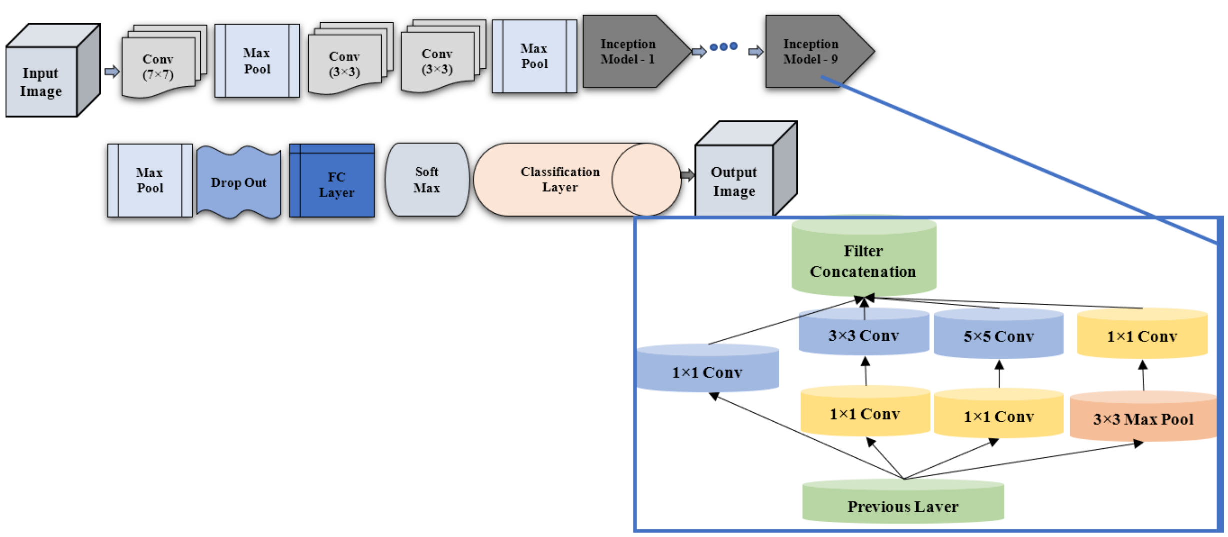

Figure 10. The architecture of GoogLeNet. [71].

The inception modules in the architecture allow simultaneous realization of multicore convolution and maximum pooling processes in one layer. This makes training of the network with optimum weights and selection of more appropriate features possible [72]. In each starting layer has 1 × 1, 3 × 3, and 5 × 5 sized convolutional layers and uses an extra 3 × 3 maximum pooling layer that can extract more distinguishing features than the ones extracted at the previous layer [71].

3.8. VGG-19

The architecture of the VGG-19 network has 24 layers, as shown in Figure 11. The architecture of VGG-19 network contains 24 layers. Sixteen convolutional layers have filters of 3 × 3 size, and these layers reduce the filter parameters. In addition to these layers, the architecture of VGG-19 network contains five pooling and three fully connected layers [73].

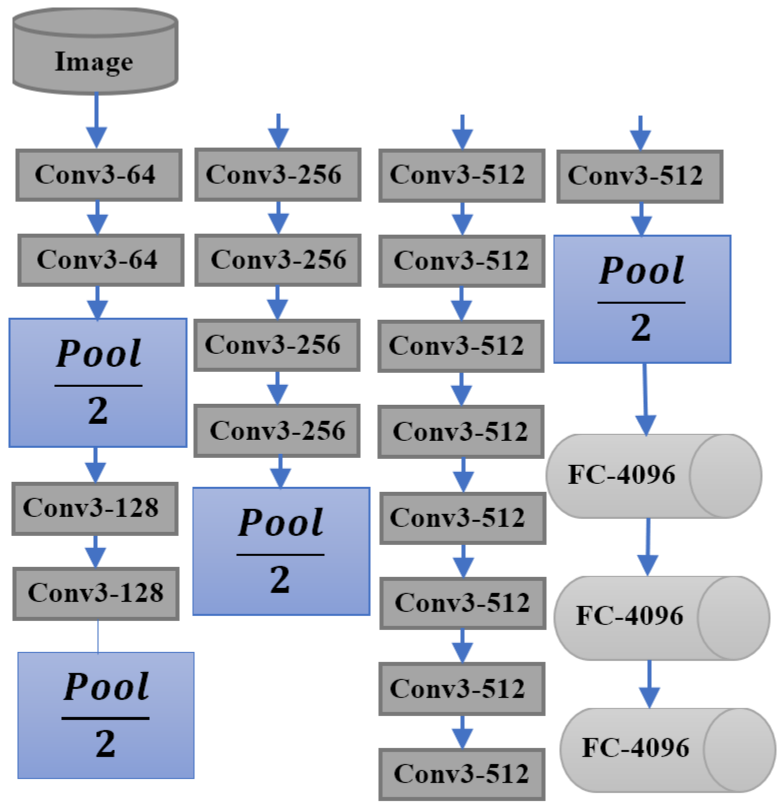

Figure 11. The structure of VGG-19 network [32].

4. Simulation results and performance evaluation

In the paper, two different workgroups were constructed. For each group, three different experiments were conducted. Furthermore, two different data sets were constructed for each group. The data set of the first group only contains images of phase portraits of Lorenz and Rössler chaotic systems. The data set of the second group only includes images of phase portraits of Lorenz and Chen chaotic systems. The images of phase portraits of xy coordinates in each group were classified. Then the images of the phase portraits of yz and xz coordinates were classified, and their classification performances were assessed. The first data set contains 600 images of xy, xz and yz phase portraits of Lorenz system and 600 images of xy, xz and yz phase portraits of Rössler system. The classification tests were conducted on these total 1200 images using pretrained networks. The second data set contains 600 images of xy, xz and yz phase portraits of Lorenz system and 720 images of xy, xz and yz phase portraits of Chen system. The classification tests were conducted on these total 1320 images using pretrained networks. The used dataset can be seen in Table 3.

Table 3. The used dataset.

	Lorenz			**Chen**			**Rössler**			**Total**
	xy	**xz**	**yz**	**xy**	**xz**	**yz**	**xy**	**xz**	**yz**	
Training (%70)	420	420	420	504	504	504	420	420	420	4032
Test (%30)	180	180	180	216	216	216	180	180	180	1728
Total	600	600	600	720	720	720	600	600	600	5760

In the study, numerous pretrained networks were utilized for the classification tests, and the eight pretrained networks with the highest performance were selected. These networks are Squeezenet, VGG-19, AlexNet, ResNet50, ResNet101, DenseNet201, ShuffleNet, and GoogLeNet. The purpose here is to compare performance results of classification of similar chaotic systems like Lorenz-Chen systems and classification of very different chaotic systems like Lorenz-Rössler systems over their images of phase portraits using deep neural networks.

4.1. Evaluation of results and performance of Lorenz-Rössler and Chen-Rössler systems classification

In this experimental group, the classifications of Lorenz-Rössler and Chen-Rössler systems are performed over two dimensional xy, yz and xz phase portraits. Some sample images of used xy, yz and xz phase portraits of Lorenz, Rössler and Chen systems are shown in Figure 12.

As it can be seen in Figure 12, the images of xy, yz and xz phase portraits of Lorenz-Rössler and Chen-Rössler systems are very different from each other. So, the classification of Lorenz-Rössler and the classification of Chen-Rössler are simple problems for the used transfer learning models. Thus, all the pretrained networks classify these phase portraits with 100% accuracy.

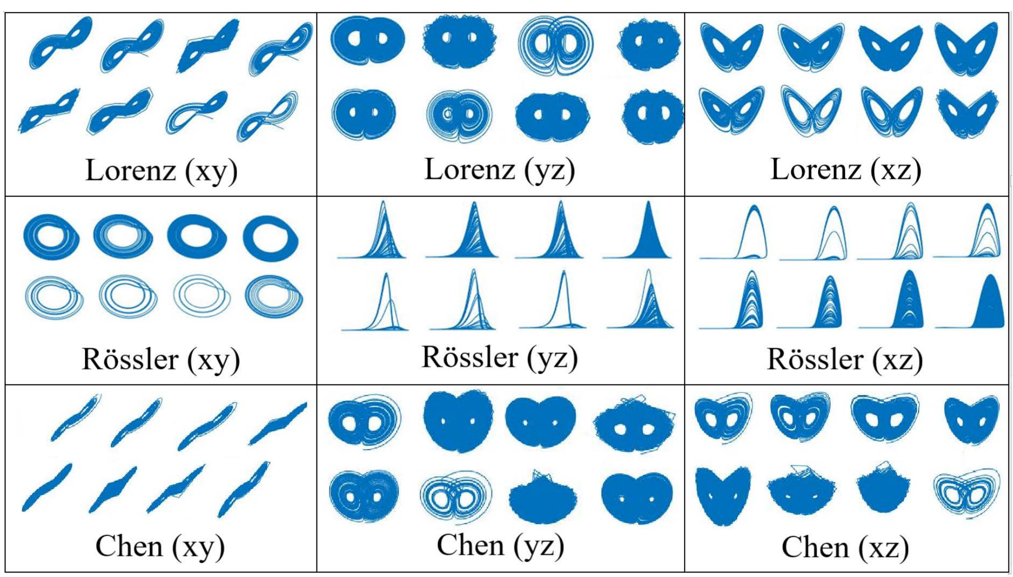

Figure 12. Sample images of phase portraits obtained from Lorenz and Rössler systems.

4.2. Evaluation of results and performance of Lorenz-Chen systems classification

In this experimental group, as second and more difficult problem, Lorenz and Chen systems are classified. Some sample images of phase portraits of Lorenz and Chen systems in Figure 13. As it is seen in Figures 13, the xy phase portraits of Lorenz and Chen systems are very alike. This makes the classification of these phase portraits very difficult. However, very good classification performance results were observed because of the preferred pretrained networks and the optimizations done for these networks. In Table 4, the contrast matrices for the xy phase portraits images are given in Figure 13. The classification performance of the pretrained networks is seen clearly in Table 4. In Table 5, the performance metrics of the classification of the xy phase portraits of Lorenz and Chen systems are given. According to Table 5, all the network has 100% performance. Because the xy phase porter images of the Lorenz and Chen systems are so dissimilar, all pretrained networks used in the study were successfully classified, as shown in Table 4. Because the xz phase portrait images of the Lorenz and Chen systems are so similar, all algorithms have successfully classified between 92 and 100 percent of the time in Table 6. Pretrained networks ResNet101 and DenseNet201 outperformed other networks in classification and correctly predicted all classes. This is because DenseNet and ResNet architectures have more features than other pretrained network architectures because they use concatenation layers instead of aggregating layers. As a result, the performance of these two networks is significantly better than that of the others. Because the yz phase portrait images of the Lorenz and Chen systems are so dissimilar in Table 7, the overall performance of all pretrained networks is around 90%–97%. DenseNet, with a success rate of 97.47 percent, is once again the most successful network.

Table 4. Contrast matrices of classification over xy phase portraits of Lorenz and Chen systems.

Network	True positive (TP)	True negative (TN)	False positive (FP)	False negative (FN)
SqueezeNet	216	180	0	0
VGG-19	216	180	0	0
AlexNet	216	180	0	0
ResNet50	216	180	0	0
ResNet101	216	180	0	0
DenseNet201	216	180	0	0
ShuffleNet	216	180	0	0
GoogLeNet	216	180	0	0

Table 5. Performance metrics of classification over xy phase portraits of Lorenz and Chen systems.

Network	Accuracy	Precision	Sensitivity	Specificity
SqueezeNet	1.000000	1.000000	1.000000	1.000000
VGG-19	1.000000	1.000000	1.000000	1.000000
AlexNet	1.000000	1.000000	1.000000	1.000000
ResNet50	1.000000	1.000000	1.000000	1.000000
ResNet101	1.000000	1.000000	1.000000	1.000000
DenseNet201	1.000000	1.000000	1.000000	1.000000
ShuffleNet	1.000000	1.000000	1.000000	1.000000
GoogLeNet	1.000000	1.000000	1.000000	1.000000

In the second experimental study carried out for this group, classification of images xz phase portraits of Lorenz and Chen systems is performed. Some sample images of xz phase portraits of Lorenz and Chen systems are shown in Figure 13. As seen in Figure 13, the xz phase portraits of Lorenz and Chen systems are very alike.

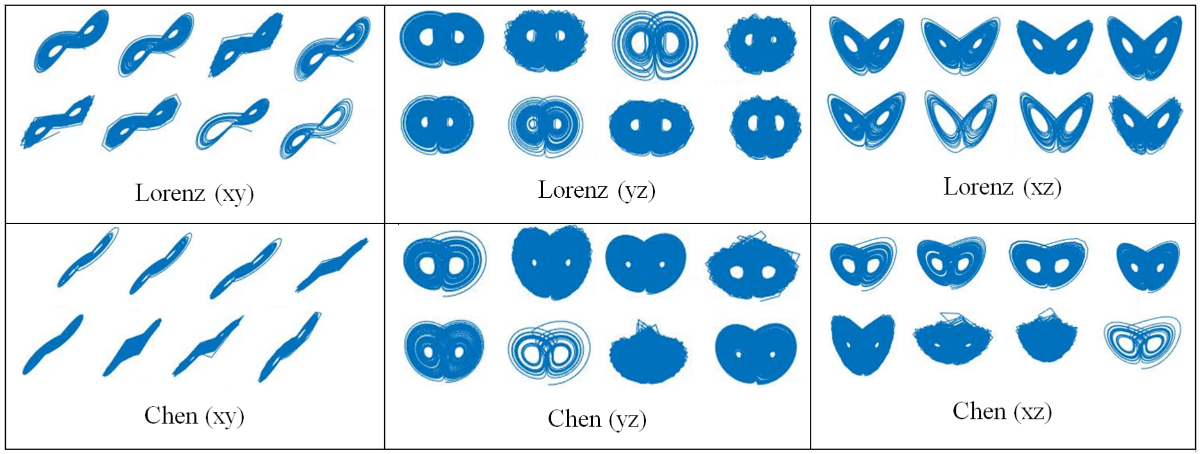

Figure 13. Sample images of phase portraits obtained from Lorenz and Chen systems.

This makes the classification of these phase portraits very difficult. However, very good classification performance results were observed because of the preferred pretrained networks and the optimizations done for these networks. In Table 6, the contrast matrices for the xz phase portraits images are given in Figure 13. The classification performance of the pretrained networks is seen clearly in Table 6.

Table 6. Contrast matrices of classification over xz phase portraits of Lorenz and Chen ystems.

Network	True positive (TP)	True negative (TN)	False positive (FP)	False negative (FN)
SqueezeNet	178	216	2	0
VGG-19	179	216	1	0
AlexNet	179	216	1	0
ResNet50	179	216	1	0
ResNet101	180	216	0	0
DenseNet201	180	216	0	0
ShuffleNet	151	216	29	0
GoogLeNet	156	216	24	0

In Table 7, the performance metrics of the classification of the xz phase portraits of Lorenz and Chen systems are given. According to Table 7, ResNet101 and DenseNet201 provide the best classification performance.

In the last experimental study for this group, the classification of images yz phase portraits of Lorenz and Chen systems is performed. Some sample images of yz phase portraits of Lorenz and Chen systems are shown in Figure 13. As seen in Figure 13, the yz phase portraits of Lorenz and Chen systems are very alike. This makes the classification of these phase portraits very difficult. However, very good classification performance results were observed because of the preferred pretrained networks and the optimizations done for these networks. In Table 8, the contrast matrices for the yz phase portraits images are given in Figure 13. The classification performance of the pretrained networks is seen clearly in Table 8.

Table 7. Performance metrics of classification over xz phase portraits of Lorenz and Chen systems.

Network	Accuracy	Precision	Sensitivity	Specificity
SqueezeNet	0.994949	0.988889	1.000000	0.990826
VGG-19	0.997475	0.994444	1.000000	0.995392
AlexNet	0.997475	0.994444	1.000000	0.995392
ResNet50	0.997475	0.994444	1.000000	0.995392
ResNet101	1.000000	1.000000	1.000000	1.000000
DenseNet201	1.000000	1.000000	1.000000	1.000000
ShuffleNet	0.926768	0.838889	1.000000	0.881633
GoogLeNet	0.939394	0.866667	1.000000	0.900000

Table 8. Contrast matrices of classification over yz phase portraits of Lorenz and Chen systems.

Network	True positive (TP)	True negative (TN)	False positive (FP)	False negative (FN)
SqueezeNet	141	216	39	0
VGG-19	180	201	0	15
AlexNet	176	198	4	18
ResNet50	179	199	1	17
ResNet101	167	211	13	5
DenseNet201	172	214	8	2
ShuffleNet	176	191	4	25
GoogLeNet	179	195	1	21

In Table 9, the performance metrics of the classification of the yz phase portraits of Lorenz and Chen systems are given. According to Table 9, DenseNet201 and VGG-19 provide the best classification performance.

Table 9. Performance metrics of classification over yz phase portraits of Lorenz and Chen systems.

Network	Accuracy	Precision	Sensitivity	Specificity
SqueezeNet	0.901515	0.783333	1.000000	0.847059
VGG-19	0.962121	1.000000	0.923077	1.000000
AlexNet	0.944444	0.977778	0.907216	0.980198
ResNet50	0.954545	0.994444	0.913265	0.995000
ResNet101	0.954545	0.927778	0.970930	0.941964
DenseNet201	0.974747	0.955556	0.988506	0.963964
ShuffleNet	0.926768	0.977778	0.875622	0.979487
GoogLeNet	0.944444	0.994444	0.895000	0.994898

In addition to the 2-way classifier, the phase portraits of these three systems can be classified at once with the 3-way classifier. For this purpose, the images in the data set were defined as three different classes, and the results in Tables 10–12, respectively, xy, xz and yz, were obtained from the models obtained as a result of the trainings made accordingly. According to these results, the best result in the classification of xy phase portraits in Table 10 was obtained with AlexNet and ResNet101. In Table 11, the best result in the classification of xz phase portraits was obtained with DenseNet201. Finally, in Table 12, the best result in the classification of yz phase portraits was obtained with AlexNet. When the obtained results are examined, it is seen that classification can be made with a sufficiently high accuracy with the 3-way classifier application. On the other hand, it is seen that the results obtained with the 2-way classifier are better as expected.

The obtained results show that transfer Learning models can effectively classify the chaotic systems over phase portraits images in this study. However, a similar classification application can also be performed with machine learning algorithms. In [22], the classification application of the same chaotic systems was carried out with machine learning methods, and the best performance was obtained with the k-nearest neighbor (KNN) algorithm with 99.20%. On the other hand, in this study, 100% accuracy was obtained with transfer learning models with 2-ways classifiers and 99.82% with 3-ways classifiers, and better results than machine learning were demonstrated.

Table 10. Performance metrics of classification over xy phase portraits of Lorenz, Chen and Rössler systems.

Network	**Accuracy**	**Precision**	**Sensitivity**	**Specificity**
SqueezeNet	0.98090	0.98385	0.97963	0.98981
VGG-19	0.99132	0.99099	0.99228	0.99579
AlexNet	0.99826	0.99816	0.99815	0.99916
ResNet50	0.98264	0.98525	0.98148	0.99074
ResNet101	0.99826	0.99846	0.99815	0.99907
DenseNet201	0.99132	0.99246	0.99074	0.99537
ShuffleNet	0.94444	0.94886	0.94074	0.97290
GoogLeNet	0.98958	0.99099	0.98889	0.99444

Table 11. Performance metrics of classification over xz phase portraits of Lorenz, Chen and Rössler systems.

Network	**Accuracy**	**Precision**	**Sensitivity**	**Specificity**
SqueezeNet	0.90799	0.92418	0.90741	0.95539
VGG-19	0.99306	0.99359	0.99259	0.99638
AlexNet	0.98958	0.98925	0.99074	0.99495
ResNet50	0.99653	0.99694	0.99630	0.99815
ResNet101	0.98090	0.98385	0.97963	0.98981
DenseNet201	0.99826	0.99816	0.99846	0.99916
ShuffleNet	0.89931	0.92944	0.89259	0.94630
GoogLeNet	0.89583	0.92754	0.88889	0.94444

Table 12. Performance metrics of classification over yz phase portraits of Lorenz, Chen and Rössler systems.

Network	**Accuracy**	**Precision**	**Sensitivity**	**Specificity**
SqueezeNet	0.83681	0.88564	0.85494	0.92088
VGG-19	0.89757	0.91633	0.90864	0.95025
AlexNet	0.94271	0.95033	0.94043	0.96987
ResNet50	0.91146	0.92641	0.92130	0.95707
ResNet101	0.89583	0.92578	0.88889	0.94461
DenseNet201	0.87847	0.90956	0.87160	0.93552
ShuffleNet	0.84549	0.88157	0.86142	0.92475
GoogLeNet	0.88021	0.90763	0.89352	0.94192

5. Conclusion

In this study, a very high accuracy classification of three different chaotic systems was performed over their phase portrait images using deep learning models for the first time in the literature. The phase portraits of the three most common chaotic systems, namely Lorenz, Chen and Rössler systems, were used to classify. All the phase portraits are obtained by numerically solving the chaotic systems with the RK4 algorithm. The numerical solutions are carried out for different step size values, initial conditions, system parameters and time range to populate the dataset with diversified data. The data set contains 6750 different phase portrait images. Classifications with very high performance are conducted utilizing SqueezeNet, VGG-19, AlexNet, ResNet50, ResNet101, DenseNet201, ShuffleNet, and GoogLeNet methods. Especially, very good classification performance results are obtained for Lorenz and Chen systems whose phase portraits, time series and dynamical properties are very alike. For all the eight networks, relatively high classification performances are observed.

The classification of the chaotic systems with different dynamical properties and time series and phase portraits like Lorenz and Rössler chaotic systems has very high-performance results as expected. For all the eight networks, relatively high classification performances are observed.

Moreover, for more difficult problem as classification of Lorenz and Chen systems, very high classification accuracy rates between 97% and 100% are achieved with AlexNet, DenseNet201 and SqueezeNet networks. Also, classification of 3 systems was also carried out using 3-ways classifier in one time, and results were obtained with a high accuracy of 99.82%. This study shows that the chaotic systems can be classified with very high accuracy over phase portraits using deep learning. Thus, this study proves that classifying real-life chaotic or random varying signals/data or associating them with a mathematical model over their phase portrait images is possible.

References

[1] Aricioglu B, Uzun S, Kacar S. Deep learning based classification of time series of Chen and Rossler chaotic systems over their graphic images. Physica D: Nonlinear Phenomena 2022; 435:133306. doi: 10.1016/j.physd.2022.133306

[2] Dokoumetzidis A, Iliadis A, Macheras P. Nonlinear Dynamics and Chaos Theory: Concepts and Applications Relevant to Pharmacodynamics. Pharmaceutical Research 2001; 18: 415–426. doi:10.1023/A:1011083723190

[3] Hilborn RC. Chaos and Nonlinear Dynamics: An Introduction for Scientists and Engineers (second ed.). Oxford University Press, 2000.

[4] Lü J, Chen G, Cheng D, Celikovsky S. Bridge the gap between the Lorenz system and the Chen system. International Journal of Bifurcation and Chaos in Applied Sciences and Engineering 2002; 12 (12): 2917-2926. doi: 10.1142/S021812740200631X

[5] Lü J, Zhou T, Chen G, Zhang S. Local bifurcations of the Chen system. International Journal of Bifurcation and Chaos 2002; 12 (10): 2257-2270. doi: 10.1142/S0218127402005819

[6] Pehlivan I, Uyaroğlu Y. Simplified chaotic diffusionless Lorenz attractor and its application to secure communication systems. IET Communication 2007; 1 (5): 1015–1022. doi: 10.1049/iet-com:20070131

[7] Sheela S, Sathyanarayana SV. Application of chaos theory in data security-a survey. Accents Transactions on Information Security 2017; 2 (5): 1-15. doi: 10.19101/TIS.2017.2500

[8] Kumar RR, Pandian R, Jacob, TP, Pravin A, Indumathi P. Cryptography Using Chaos In Communication Systems. In Journal of Physics: Conference Series 2021; 1 (1770): 12-96. doi:10.1088/1742-6596/1770/1/012096

[9] Albahrani EA, Alshekly TK, Lafta SH. A Review on Audio Encryption Algorithms Using Chaos Maps-Based Techniques. Journal of Cyber Security and Mobility 2022; 11 (1): 53-82. doi: 10.13052/jcsm2245-1439.1113

[10] Karmakar J, Pathak A, Nandi D, Mandal MK. Sparse representation based compressive video encryption using hyper-chaos and DNA coding. Digital Signal Processing 2021; 117 (103143): 1-14. doi: 10.1016/j.dsp.2021.103143

[11] Chen D, Shi S, Gu X, Shim, B. Weak Signal Frequency Detection Using Chaos Theory: A Comprehensive Analysis. IEEE Transactions on Vehicular Technology 2021; 9 (70): 8950-8963. doi: 10.1109/TVT.2021.3098710

[12] Wu H, Yin Z, Xie, J, Ding, P, Liu, P, Song, H, Zhang, Y. Design and implementation of true random number generators based on semiconductor superlattice chaos. Microelectronics Journal 2021; 114 (105119): 1-7. doi: 10.1016/j.mejo.2021.105119

[13] Hematpour N, Ahadpour S, Behnia S. Presence of dynamics of quantum dots in the digital signature using DNA alphabet and chaotic S-box. Multimedia Tools and Applications 2021; 80 (7): 10509-10531. doi: 10.1007/s11042-020-10059-5

[14] Di Bernardo M, Garefalo F, Glielmo L, Vasca F. Switchings, bifurcations, and chaos in DC/DC converters. IEEE Transactions on Circuits and Systems I: Fundamental Theory and Applications 1998; 45 (2): 133-141. doi: 10.1109/81.661675

[15] Sarker IH. Deep learning: a comprehensive overview on techniques, taxonomy, applications and research directions. SN Computer Science 2021; 2 (6): 1-20. doi: 10.1007/s42979-021-00815-1

[16] Kaya U, Yılmaz A, Dikmen Y. Deep Learning Methods used in the field of Health. European Journal of Science and Technology 2019; 16: 792–808. doi: 10.31590/ejosat.573248

[17] Barros P, Parisi GI, Weber C, Wermter S. Emotion-modulated attention improves expression recognition: A deep learning model. Neurocomputing 2017; 253: 104–114. doi: 10.1016/j.neucom.2017.01.096

[18] Rakhlin A, Shvets A, Iglovikov V, Kalinin AA. Deep Convolutional Neural Networks for Breast Cancer Histology Image Analysis. Lecture Notes in Computer Science 2018; 10882: 737–744. doi: 10.1007/978-3-319-93000-8_83

[19] Zhang Y, Pezeshki M, Brakel P, Zhang S, Laurent C, et al. Towards End-to-End Speech Recognition with Deep Convolutional Neural Networks. Proceedings Interspeech 2016; 410-414. doi: 10.48550/arXiv.1701.02720

[20] Qian Y, Bi M, Tan T, Yu K. Very Deep Convolutional Neural Networks for Noise Robust Speech Recognition. IEEE/ACM Transactions on Audio, Speech, and Language Processing 2016; 24 (12): 2263–2276. doi: 10.1109/TASLP.2016.2602884

[21] Young T, Hazarika D, Poria S, Cambria E. Recent trends in deep learning based natural language processing. IEEE Computational Intelligence Magazine 2018; 13 (3): 55–75. doi: 10.1109/MCI.2018.2840738

[22] Conneau A Schwenk H Barrault L, Lecun Y. Very deep convolutional networks for natural language processing. arXiv preprint arXiv:1606.01781 2016; 2 (1): 1-9.

[23] Deng L, Liu Y. Deep Learning in Natural Language Processing. Singapore: Springer, 2018.

[24] Toraman S. Pedestrian Detection with Deep Learning from Unmanned Aerial Imagery. Journal of Aviation 2018; 2 (2): 64–69.

[25] Altan G. DeepGraphNet: Deep Learning Models in the Classification of Graphs. European Journal of Science and Technology 2019; 319–327. doi:10.31590/ejosat.638256

[26] Boulle N, Dallas V, Nakatsukasa Y, Samaddar D. Classification of chaotic time series with deep learning. Physica D: Nonlinear Phenomena 2020; 403: 132261. doi: 10.1016/j.physd.2019.132261

[27] Uzun S. Machine learning-based classification of time series of chaotic systems. The European Physical Journal Special Topics 2022; 231: 493-503. doi: 10.1140/epjs/s11734-021-00346-z

[28] Yeo K. Model-free prediction of noisy chaotic time series by deep learning. arXiv:1710.01693v1 2017; doi: 10.48550/arXiv.1710.01693

[29] Kuremoto T, Obayashi M, Kobayashi K, Hirata T, Mabu S. Forecast chaotic time series data by DBNs. In: 7th International Congress on Image and Signal Processing - CISP 2014; Dalian, China; 2014. pp. 1130–1135.

[30] Sangiorgio M, Dercole F. Robustness of LSTM neural networks for multi-step forecasting of chaotic time series. Chaos, Solitons and Fractals 2020; 139: 110045. doi: 10.1016/j.chaos.2020.110045

[31] Iandola FN, Han S, Moskewicz MW, Ashraf K, Dally WJ. SqueezeNet: AlexNet-level accuracy with 50x fewer parameters and< 0.5 MB model size. arXiv preprint arXiv:1602.07360v4 2016. doi: 10.48550/arXiv.1602.07360

[32] Wen L, Li X, Li X, Gao L. A new transfer learning based on VGG-19 network for fault diagnosis. In: IEEE 23rd International Conference on Computer Supported Cooperative Work in Design - CSCWD; Porto, Portugal; 2019. pp. 205–209.

[33] Lu S, Lu Z, Zhang YD. Pathological brain detection based on AlexNet and transfer learning. Journal of Computational Science 2019; 30: 41–47. doi: 10.1016/j.jocs.2018.11.008

[34] He K, Zhang X, Ren S, Sun J. Deep Residual Learning for Image Recognition. In: IEEE Conference on Computer Vision and Pattern Recognition (CVPR); Las Vegas, NV, USA; 2016. pp. 770–778.

[35] Behzadi M, Safabakhsh R. Text Detection in Natural Scenes using Fully Convolutional DenseNets. In: 4th Iranian Conference on Signal Processing and Intelligent Systems (ICSPIS); Tehran, Iran; 2018. pp. 11–14.

[36] Zhang X, Zhou X, Lin M, Sun J. ShuffleNet: An Extremely Efficient Convolutional Neural Network for Mobile Devices. In: The IEEE Computer Society Conference on Computer Vision and Pattern Recognition; Salt Lake City, UT, USA; 2018. pp. 6848–6856.

[37] Russakovsky O, Deng J, Su H, Krause J, Satheesh S et al. ImageNet Large Scale Visual Recognition Challenge. International Journal of Computer Vision 2015; 115: 211–252. doi: 10.1007/s11263-015-0816-y

[38] Yu P, Xu F. A common phenomenon in chaotic systems linked by time delay. International Journal of Bifurcation and Chaos 2006; 16 (12): 3727-3736. doi: 10.1142/S0218127406017129

[39] Lorenz EN. Deterministic nonperiodic flow. Journal of the Atmospheric Sciences 1963; 20 (2): 130-141. doi: 10.1175/1520-0469(1963)020<0130:DNF>2.0.CO;2

[40] Pehlivan I, Uyaroğlu Y. A new chaotic attractor from general Lorenz system family and its electronic experimental implementation. Turkish Journal of Electrical Engineering & Computer Sciences 2010; 18 (2): 171–184. doi:10.3906/elk-0906-67

[41] Gorman M, Widmann PJ, Robbins LA. Nonlinear dynamics of a convection loop: A quantitative comparison of experiment with theory. Physica D: Nonlinear Phenomena 1986; 19 (2): 255–267. doi: 10.1016/0167-2789(86)90022-9

[42] Haken H. Analogy between higher instabilities in fluids and lasers. Physics Letters A 1975; 53 (1): 77–78. doi: 10.1016/0375-9601(75)90353-9

[43] Cuomo KM, Oppenheim AV. Circuit implementation of synchronized chaos with applications to communications. Physical Review Letters 1993; 71 (1): 65–68. doi: 10.1103/PhysRevLett.71.65

[44] Hemati N. Strange Attractors in Brushless DC Motors. IEEE Transactions on Circuits and Systems I: Fundamental Theory and Applications 1994; 41 (1): 40–45. doi: 10.1109/81.260218

[45] Knobloch E. Chaos in the segmented disc dynamo. Physics Letters A 1981; 82 (9): 439–440. doi: 10.1016/0375-9601(81)90274-7

[46] Chen G, Ueta T. Yet another chaotic attractor. International Journal of Bifurcation and Chaos 1999; 9 (7): 1465–1466. doi: 10.1142/S0218127499001024

[47] Lozi R, Pchelintsev AN. A New Reliable Numerical Method for Computing Chaotic Solutions of Dynamical Systems: The Chen Attractor Case. International Journal of Bifurcation and Chaos 2015; 25 (13): 1550187. doi: 10.1142/S0218127415501874

[48] Rössler OE. An equation for continuous chaos. Physics Letters A 1976; 57 (5): 397–398. doi: 10.1016/0375-9601(76)90101-8

[49] Altun K, Günay E. A novel chaos-based modulation scheme: Adaptive threshold level chaotic on-off keying for increased BER performance. Turkish Journal of Electrical Engineering & Computer Sciences 2020; 28 (2): 606–620. doi:10.3906/elk-1904-186

[50] Chapra SC, Canale RP. Numerical Methods for Engineers: with Software and Programming Applications 4th ed., McGraw-Hill, New York, 2002.

[51] Guo Y, Liu Y, Oerlemans A, Lao S, Wu S et al. Deep learning for visual understanding: A review. Neurocomputing 2016; 187: 27–48. doi: 10.1016/j.neucom.2015.09.116

[52] Haskins G, Kruger U, Yan P. Deep Learning in Medical Image Registration: A Survey. Machine Vision and Applications 2019; 31 (8): 1-18. doi:10.1007/s00138-020-01060-x

[53] Küçük D, Arıcı N. A Literature Study on Deep Learning Applications in Natural Language Processing. International Journal of Management Information Systems and Computer Science 2018; 2 (2): 76–86.

[54] Keleş A. Deep Learning and Applications in Health. Journal of Turkish Studies 2018; 13 (21): 113–127. doi: 10.7827/TurkishStudies.14189

[55] LeCun Y, Bottou L, Bengio Y, Haffner P. Gradient-based learning applied to document recognition. Proceedings of the IEEE 1998; 86 (11): 2278–2323. doi: 10.1109/5.726791

[56] LeCun Y, Jackel LD, Boser B, Denker JS, Graf HP et al. Handwritten digit recognition: applications of neural net chips and automatic learning. Neurocomputing 1990; 303-318. doi: 10.1007/978-3-642-76153-9_35

[57] Ravi D, Wong C, Deligianni F, Berthelot M, Andreu-Perez J et al. Deep Learning for Health Informatics. IEEE Journal of Biomedical and Health Informatics 2017; 21 (1): 4–21. doi: 10.1109/JBHI.2016.2636665

[58] Zheng Z, Zhang H, Li X, Liu S, Teng Y. ResNet-Based Model for Cancer Detection. In: IEEE International Conference on Consumer Electronics and Computer Engineering-ICCECE; 2021. pp. 325–328.

[59] Zahisham Z, Lee CP, Lim KM. Food Recognition with ResNet-50. In: IEEE International Conference on Artificial Intelligence in Engineering and Technology-IICAIET; Guangzhou, China; 2020. pp. 1–5.

[60] Talo M. Classification of Histopathological Breast Cancer Images using Convolutional Neural Networks. Fırat University Journal of Engineering Science 2019; 31 (2): 391–398. doi: 10.35234/fumbd.517939

[61] Aksoy B, Halis HD, Salman OKM. Identification of Diseases in Apple Plants with Artificial Intelligence Methods and Comparison of the Performance of Artificial Intelligence Methods. International Journal of Engineering and Innovative Research 2020; 2(3): 194–210. doi: 10.47933/ijeir.772514

[62] Krizhevsky A, Sutskever I, Hinton GE. ImageNet Classification with Deep Convolutional Neural Networks. Communications of the ACM 2017; 60 (6): 84–90.

[63] Gonzalez TF. Handbook of Approximation Algorithms and Metaheuristics. New York, USA: Chapman and Hall/CRC, 2007.

[64] Ballester P, Araujo RM. On the performance of googlenet and alexnet applied to sketches. In: 30th AAAI Conference on Artificial Intelligence-AAAI; North America; 2016. pp. 1124–1128.

[65] Han X, Zhong Y, Cao L, Zhang L. Pre-Trained AlexNet Architecture with Pyramid Pooling and Supervision for High Spatial Resolution Remote Sensing Image Scene Classification. Remote Sensing 2017; 9 (8): 848. doi: 10.3390/rs9080848

[66] Huang G, Liu Z, Van Der Maaten L, Weinberger KQ. Densely Connected Convolutional Networks. In: IEEE Conference on Computer Vision and Pattern Recognition (CVPR); Honolulu, HI, USA; 2017. pp. 2261–2269.

[67] Yilmaz F, Kose O, Demir A. Comparison of two different deep learning architectures on breast cancer. In: Medical Technologies Congress (TIPTEKNO); Izmir, Turkey; 2019. pp. 1–4.

[68] Zhang K, Guo Y, Wang X, Yuan J, Ma Z et al. Channel-Wise and Feature-Points Reweights Densenet for Image Classification. In: IEEE International Conference on Image Processing (ICIP); Taipei, Taiwan 2019; 410–414.

[69] Chen C, Zhu T, Li S, Liu B. Apple Leaf Disease Regcognition Method Base on Improved ShuffleNet V2. In: 3rd International Conference on Advances in Computer Technology, Information Science and Communication (CTISC); Shanghai, China 2021;276–282.

[70] Szegedy C, Liu W, Jia Y, Sermanet P, Reed S et al. Going deeper with convolutions. In: The IEEE Computer Society Conference on Computer Vision and Pattern Recognition; Boston, MA; 2015; 1–9.

[71] Balagourouchetty L, Pragatheeswaran JK, Pottakkat B, Ramkumar G. GoogLeNet-Based Ensemble FCNet Classifier for Focal Liver Lesion Diagnosis. IEEE Journal of Biomedical and Health Informatics 2020; 24 (6): 1686–1694. doi: 10.1109/JBHI.2019.2942774

[72] Zhu Z, Li J, Zhuo L, Zhang J. Extreme Weather Recognition Using a Novel Fine-Tuning Strategy and Optimized GoogLeNet. In: International Conference on Digital Image Computing: Techniques and Applications - DICTA; Sydney, NSW, Australia; 2017. pp. 1–7.

[73] Toğaçar M, Ergen B, Özyurt F. Classification of Flower Images by Using Feature Selection Methods in Convolutional Neural Network Models. Fırat University Journal of Engineering Science 2020; 32 (1): 47 - 56. doi: 10.35234/fumbd.573630